Oncogene (2010) 29, 5146–5158

www.nature.com/onc

ORIGINAL ARTICLE

AZGP1 is a tumor suppressor in pancreatic cancer inducing mesenchymal-to-epithelial transdifferentiation by inhibiting TGF-β-mediated ERK signaling

B Kong[1,3], CW Michalski[1,3], X Hong[1], N Valkovskaya[1], S Rieder[1], I Abiatari[1], S Streit[1], M Erkan[1], I Esposito[2], H Friess[1] and J Kleeff[1]

[1]*Department of Surgery, Technische Universität München, Munich, Germany and* [2]*Institute of Pathology, Technische Universität München, Munich, Germany*

Epithelial-to-mesenchymal transdifferentiation (EMT) mediated by transforming growth factor-β (TGF-β) signaling leads to aggressive cancer progression. In this study, we identified zinc-α2-glycoprotein (AZGP1, ZAG) as a tumor suppressor in pancreatic ductal adenocarcinoma whose expression is lost due to histone deacetylation. *In vitro*, ZAG silencing strikingly increased invasiveness of pancreatic cancer cells accompanied by the induction of a mesenchymal phenotype. Expression analysis of a set of EMT markers showed an increase in the expression of mesenchymal markers (vimentin (VIM) and integrin-α5) and a concomitant reduction in the expression of epithelial markers (cadherin 1 (CDH1), desmoplakin and keratin-19). Blockade of endogenous TGF-β signaling inhibited these morphological changes and the downregulation of CDH1, as elicited by ZAG silencing. In a ZAG-negative cell line, human recombinant ZAG (rZAG) specifically inhibited exogenous TGF-β-mediated tumor cell invasion and VIM expression. Furthermore, rZAG blocked TGF-β-mediated ERK2 phosphorylation. PCR array analysis revealed that ZAG-induced epithelial transdifferentiation was accompanied by a series of concerted cellular events including a shift in the energy metabolism and prosurvival signals. Thus, epigenetically regulated ZAG is a novel tumor suppressor essential for maintaining an epithelial phenotype.
Oncogene (2010) **29,** 5146–5158; doi:10.1038/onc.2010.258; published online 28 June 2010

Keywords: pancreatic cancer; AZGP1; EMT; MET; transdifferentiation; transforming growth factor-β

Introduction

Zinc-α2-glycoprotein (AZGP1, ZAG) is a secreted 41-kDa protein whose function has not yet been fully elucidated. ZAG has initially been identified and purified in human serum already in 1961 (Burgi and Schmid, 1961). Using immunohistochemical studies, it has been found that ZAG is expressed mainly in epithelial cells of the breast, the prostate, the liver and various other gastrointestinal organs (Tada *et al*., 1991). In line with its production by secretory epithelial cells, ZAG is found in a number of body fluids (Frenette *et al*., 1987; Ohkubo *et al*., 1990). Recently, it has been shown that ZAG might be involved in carcinogenesis and tumor differentiation. Thus, in prostate and breast cancer, expression of ZAG has been linked to poorer tumor differentiation (Diez-Itza *et al*., 1993; Hale *et al*., 2001) though the underlying mechanisms remain elusive. ZAG has also been associated with cancer cachexia due to its high level of amino-acid sequence homology with tumor-derived lipid-mobilizing factor (Russell *et al*., 2004) and because in a mouse model of ZAG-producing tumors, ZAG stimulated lipolysis in adipocytes leading to cachexia (Bing *et al*., 2004).

Epithelial-to-mesenchymal transdifferentiation (EMT) leading to aggressive cancer progression is considered to be a crucial event in the carcinogenesis of pancreatic ductal adenocarcinoma (PDAC). EMT is characterized by the loss of epithelial characteristics and by the acquisition of a mesenchymal phenotype (Brabletz *et al*., 2005). During carcinogenesis and development of a more mesenchymal phenotype, less motile (epithelial) cells restart developmental programs (that is, transforming growth factor-β (TGF-β), notch, Wnt and hedgehog pathways) to gain migratory and invasive properties (Ellenrieder *et al*., 2001; Brabletz *et al*., 2005; Dembinski and Krauss, 2009; Wang *et al*., 2009). This involves the loss of cell–cell junctions and a reorganization of the actin cytoskeleton, as well as the acquisition of resistance to apoptosis, and thus of resistance to chemotherapy (Robson *et al*., 2006; Wang *et al*., 2009). The complexity of the underlying signaling processes and the adoption of a completely different phenotype imply that EMT is not a simple change in migratory/invasive capabilities but rather a switch into a different cellular program. Importantly, these 'features' seem to necessitate that the cell forfeits proliferative capacities to survive under anchorage-independent conditions, as recently shown in K-ras/extracellular signal-regulated kinase (ERK)-activated breast cancer

Correspondence: Dr J Kleeff, Department of Surgery, Technische Universität München, Ismaningerstrasse 22, Munich 81675, Germany. E-mail: kleeff@chir.med.tu-muenchen.de
[3]These authors contributed equally to this work.
Received 14 January 2010; revised 11 May 2010; accepted 28 May 2010; published online 28 June 2010

cells (Evdokimova *et al*., 2009). Similarly in pancreas cancer, a subpopulation of slowly dividing cancer cells show an EMT-resembling morphology (Dembinski and Krauss, 2009). On the molecular level, EMT is defined by downregulation of epithelial differentiation markers (for example, cadherin 1 (CDH1)) and by the transcriptional induction of mesenchymal markers, such as vimentin (VIM) and CDH2. In spite of its high activation threshold, EMT can be induced by members of the TGF-β family including TGF-β1 and BMP4 (Ellenrieder *et al*., 2001; Hamada *et al*., 2007). Though TGF-β is a tumor suppressor in the early stages of PDAC, it contributes to tumor progression by promoting EMT and invasion in the late cancer stages (Ellenrieder *et al*., 2001; Hamada *et al*., 2007). Constitutively active Ras signaling—as a consequence of K-ras mutations that are present in 70–90% of PDAC—has been shown to be indispensable for TGF-β-mediated induction of EMT (Longnecker and Terhune, 1998; Ellenrieder *et al*., 2001; Roberts and Wakefield, 2003; Horiguchi *et al*., 2009). These data suggest that TGF-β cooperates with Ras/ERK signaling in advanced stages of PDAC promoting invasion and metastasis through EMT. Therefore, EMT not only entails the orchestration of promigratory/invasive events but also reorganization of proliferation to allow for survival in different microenvironments. As we show ZAG to be widely lost in pancreatic cancer, we hypothesize that it might have tumor-suppressor functions and that it might be involved in EMT in PDAC.

Results

Expression of ZAG is decreased in primary and metastatic PDAC

Quantitative real-time-PCR (QRT–PCR) of bulk normal pancreatic tissues ($n=19$) and PDAC ($n=57$) tissues revealed a significant downregulation of ZAG mRNA expression in PDAC ($-6.5\times$, $P<0.0001$; Figure 1a). Though ZAG staining was predominantly detected in acinar and peripheral cells of islets in the normal pancreas (Figure 1b), its expression in normal ducts was generally absent (Supplementary Figure 1). In contrast, ZAG staining in cancer cells was lost in 74% of the PDAC cases (42/57) and only 21% (12/57) and 5% (3/57) of the samples showed moderate or strong ZAG staining intensities in cancer cells (Figure 1c, right panel). Consistent with our results, published serial analysis of gene expression data of isolated primary PDAC cells demonstrated that 50% (12/24) of cancers showed low expression of ZAG (less than 100 tags), whereas 37.5% (9/24) and 12.5% (3/24) of the cells expressed moderate (100–1000 tags) or high (more than 1000 tags) ZAG levels (Jones *et al*., 2008; Figure 1c, left panel; http://www.sciencemag.org/cgi/content/full/sci; 1164368/DC1). Moreover, 39 metastatic PDAC tissues consisting of liver metastasis (23), lymph node metastasis (6), peritoneal metastasis (6), omentum metastasis (3) and muscle metastasis (1) were stained for ZAG. Among these samples we detected, apart from two (5%) ZAG-positive liver metastases (Figure 1d, right lower panel), only ZAG-negative (Figure 1d) metastatic cancer cells. In addition, ZAG staining was performed on a tissue Pancreatic Intraepithelial Neoplasia (PanIN) array containing 44 PanIN lesions of different grades. It is of note that scattered ZAG-expressing cells were observed in 48% (21/44) of the lesions, though the appearance of such scattered ZAG-positive cells was not correlated to the grade of the lesions (Figure 1e). Comparison of the staining intensities in PanIN lesions, primary and metastatic PDAC revealed striking differences in expression levels (Figure 1f, 48 vs 26 vs 5%, $P<0.05$). As ZAG expression was mainly observed in acinar and endocrine cells in the normal pancreas, we set out to investigate its expression in pancreatic endocrine tumors (PETs) and in acinar cell carcinomas (ACCs). Although ZAG expression was detected in 50% (7/14) of the PET samples and two out of three PET cell lines (Supplementary Figures 2A and B), only 18% (2/11) of the ACC samples were positive for ZAG (Supplementary Figure 2C). Altogether, the rate of ZAG-positive cancer cells in PET was generally higher than that in PDAC and ACC (Figure 1g, 50 vs 26 and 18%).

Few cancer cell lines express and secrete ZAG

ZAG mRNA expression and ZAG protein (cell lysates and supernatants) were only found in two (Aspc-1 and Capan-1) out of seven tested cell lines (Aspc-1, Capan-1, Colo-357, Mia-PaCa-2, Panc-1, T3M4 and Su86.86; Figures 2a and b). As there are three *N*-linked glycosylation sites on human ZAG (as assessed by X-ray crystallography) (Ohkubo *et al*., 1990; Rolli *et al*., 2007), we set out to determine whether glycosylation contributes to cellular transport of ZAG. In line with this assumption, inhibition of *N*-linked glycosylation by tunicamycin significantly decreased ZAG secretion in Aspc-1 and Capan-1 cells (Figure 2c). Though there were no differences between ZAG expression and secretion in cancer cell lines, we hypothesized that secretion might be altered *in vivo* (potentially due to deglycosylation). Therefore, we measured ZAG levels in the sera of PDAC patients ($n=16$) and healthy volunteers ($n=14$) revealing no significant differences between the groups (Figure 2d).

Histone deacetylase inhibition reconstitutes ZAG expression and induces MET in pancreatic cancer cells

To assess the mechanism underlying downregulation/loss of ZAG in most of the tested PDAC cells, we performed demethylation and deacetylation-inhibition assays. Although the histone deacetylase (HDAC) inhibitor Trichostatin A (TSA) reconstituted ZAG expression in the two ZAG-negative cell lines T3M4 and Panc-1 on both the mRNA and protein levels (Figures 3a and b), demethylation using 5-aza-2′-deoxycytidine (5-aza) had no such effect (data not shown). Similar results were also obtained from two additional cell lines (Colo-357 and Su86.86), though to a lesser extent than in Su86.86 cells (Supplementary

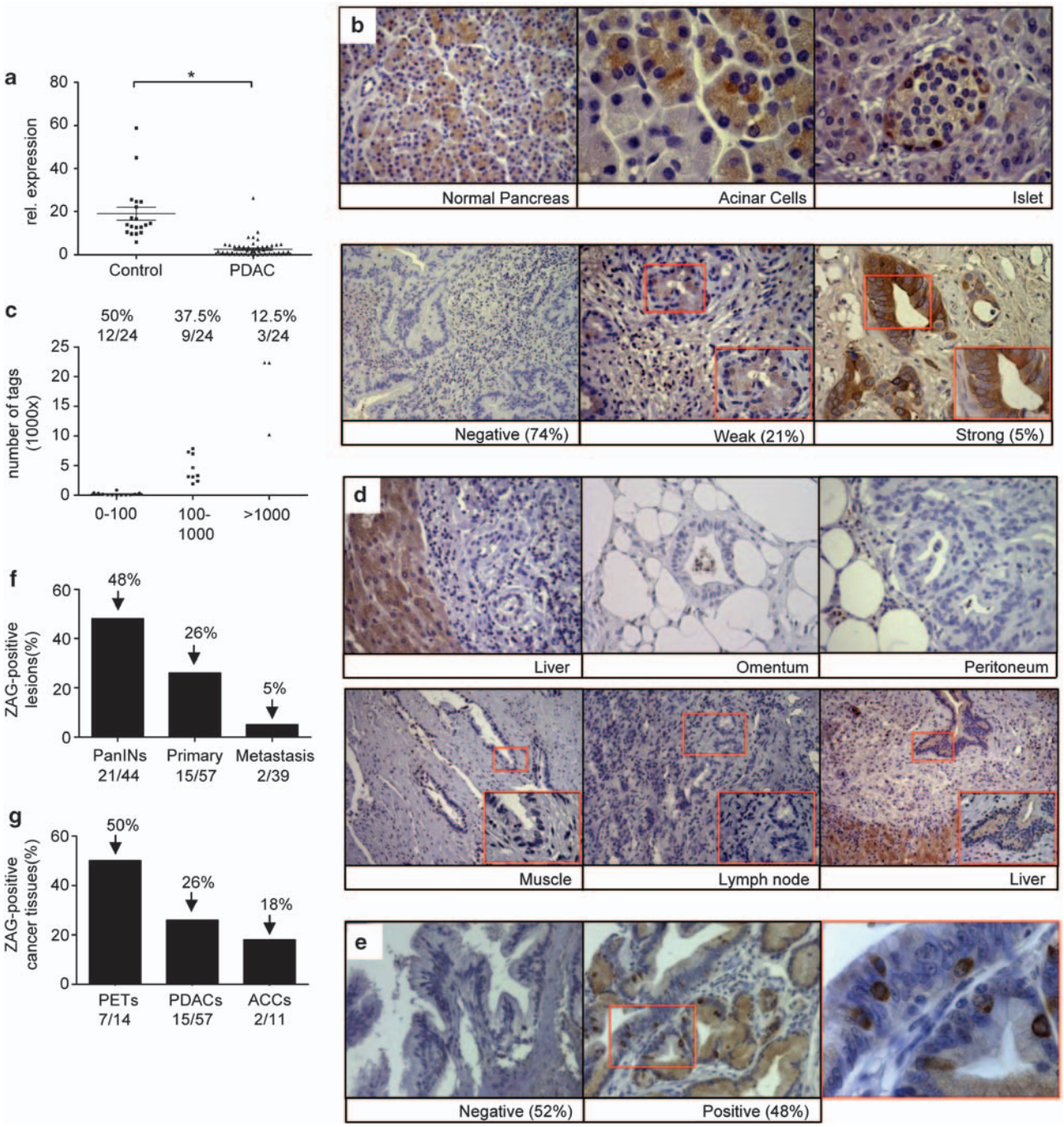

Figure 1 Expression of ZAG is decreased in primary and metastatic PDAC. (**a**) Expression of ZAG mRNA in normal pancreas ($n = 19$) and PDAC ($n = 57$) tissues was analyzed by QRT–PCR as described in the Materials and methods section. Data are presented as relative expression (normalized to the median expression of ZAG in PDAC tissues). (**b**) Normal pancreatic acinar cells and islet cells are immunopositive for ZAG (magnifications, $\times 200$, $\times 630$ and $\times 400$). (**c**) Analysis of published serial analysis of gene expression data (Jones *et al*., 2008): 50% of primary PDAC cells express low levels of ZAG, whereas 37.5 and 12.5% show moderate and high ZAG expression levels, respectively (left panel, http://www.sciencemag.org/cgi/content/full/sci;1164368/DC1). In the majority (74%) of the analyzed primary PDAC tissue sections, cancer cells are ZAG-negative, whereas 21 and 5% exhibit weak and strong staining of ZAG, respectively (right panel, $\times 200$). (**d**) In 95% of the metastatic PDAC tissue sections (liver ($\times 200$), omentum ($\times 200$), peritoneum ($\times 200$), muscle ($\times 100$) and lymph node ($\times 200$)), cancer cells are ZAG-negative (right panel). Only 5% (two liver metastases) of metastatic tissues are weakly ZAG-positive (right lower panel, $\times 100$). (**e**) ZAG-expressing cells (middle panel, $\times 200$, right panel, $\times 630$) were observed in 48% of PanIN lesions; 52% of the lesions were ZAG-negative (left panel, $\times 200$). (**f**) Immunohistochemically, the rate of ZAG-positive cells in PanIN lesions, primary and metastatic PDAC, gradually decreases from 48 to 26 and 5%. (**g**) The percentage of ZAG-positive samples in PET is generally higher than in PDAC or ACC (50 vs 26 and 18%).

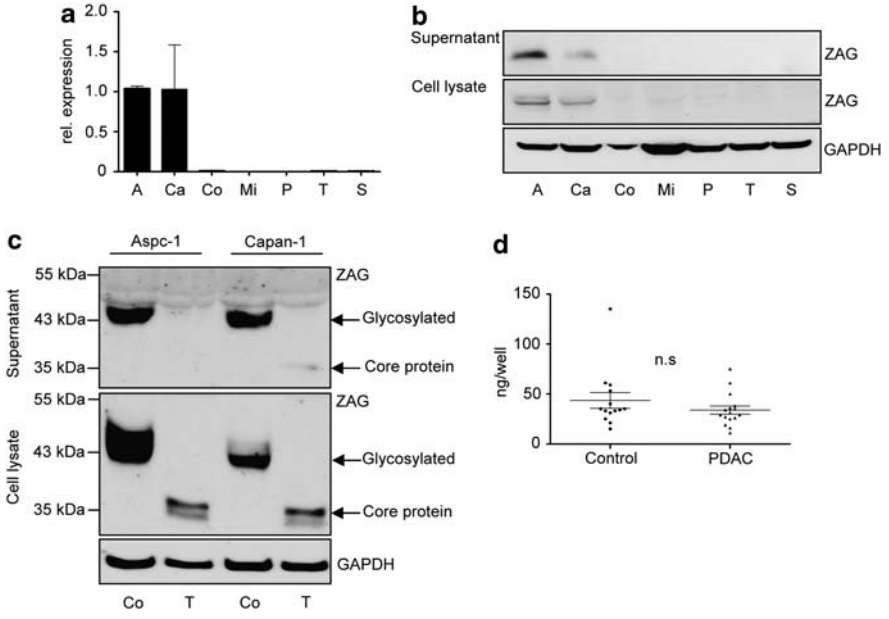

Figure 2 Few cancer cell lines express and secrete ZAG. (**a**) mRNA expression analysis (QRT–PCR) of ZAG in pancreatic cancer cell lines. Out of seven tested cell lines (Aspc-1 (A), Capan-1 (Ca), Colo357 (Co), Mia-PaCa2 (Mi), Panc-1 (P), T3M4 (T), Su86.86 (S)), only Aspc-1 and Capan-1 expressed ZAG. (**b**) Correspondingly, ZAG protein is found in both supernatants and cell lysates of Aspc-1 and Capan-1 cells by immunoblot analysis; loading control: GAPDH. (**c**) Tunicamycin treatment shifts the molecular weight of ZAG from 43 kDa (glycosylated) to 35 kDa (cell lysates) and significantly decreases ZAG levels in the supernatants of Aspc-1 and Capan-1 cells. One representative immunoblot out of two independent experiments is shown. (**d**) ZAG levels in the sera of PDAC patients ($n = 16$) and healthy volunteers ($n = 14$) were determined by enzyme-linked immunosorbent assay. No significant (NS) differences were found between the groups.

Figures 3A and B). We corroborated these findings by treating Panc-1 cells with TSA, which induced a time-dependent, increased acetylation of histone H3 (Figure 3c). Chromatin immunoprecipitation revealed a significantly increased binding of acetylated histone H3 to the ZAG promoter (Figure 3d), suggesting an open chromatin conformation within that region. As it has been shown recently that inhibition of HDAC in Panc-1 cells abolished TGF-β1-mediated EMT (Fritsche *et al*., 2009; von Burstin *et al*., 2009), we set out to determine whether inhibition of HDACs in Panc-1 cells would influence their steady-state differentiation status. To this end, we performed QRT–PCR to compare expression of a panel of EMT markers (CDH1, keratin-19 (KRT19), dentin sialoprotein (DSP), VIM and integrin-α 5) between dimethyl sulfoxide (DMSO)- and TSA-treated cells. This analysis revealed that TSA treatment induced a more epithelial-like phenotype in Panc-1 cells characterized by increased expression of epithelial markers (KRT19 and CDH1) and a concomitant downregulation of a mesenchymal marker (VIM, Figure 3e). The changes in CDH1 and VIM expression were also confirmed on the protein level (Figure 3f). Consistently, TSA treatment significantly decreased cancer cell invasion (Figure 3g, upper panel), whereas no influence on cell proliferation was observed (Figure 3g, lower panel).

ZAG inhibits invasion of pancreatic cancer cells by blocking TGF-β-mediated EMT

Though ZAG RNAi in Aspc-1 cells significantly decreased its expression (Figure 4a, left panel) compared with controls, no significant effect on cell growth was observed (Figure 4a, middle panel). Accordingly, treatment of Aspc-1 cells with human recombinant ZAG (rZAG) did not alter proliferation (Supplementary Figure 4A). However, RNAi-mediated ZAG silencing strikingly increased invasiveness of Aspc-1 cells, which was partially reversible by treatment with rZAG (though to a lesser extent when using lower concentrations of rZAG; Figure 4a, right panel). As this increase in invasiveness was accompanied by significant phenotypic changes of cellular morphology (Figure 4b, left panel; more epithelial structure of control cells vs a fibroblast-like phenotype of many siRNA-treated cells forming scattered cell clusters; confirmed by actin staining, Figure 4b), we hypothesized that ZAG RNAi might induce a mesenchymal program. Therefore, we performed QRT–PCR to the compare expression patterns of a panel of EMT markers (CDH1, KRT19, DSP, VIM, ITGA5, ITGB1, ITGAV and ITGA3) between control and ZAG-silenced Aspc-1 cells. This assay revealed that the epithelial markers CDH1, DSP and KRT19 were significantly downregulated whereas the mesenchymal markers VIM and ITGA5 were upregulated (Figure 4b, middle panel). The changes in CDH1 and VIM expression were confirmed at the protein level (Figure 4b, right panel). In addition, we validated the results of the invasion assays as well as the changes in morphology and EMT markers using two ZAG siRNA molecules (Supplementary Figures 4B and C). Because TGF-β signaling is considered to be one of the major driving forces of EMT in PDAC, we speculated that the inhibitory effect of ZAG on EMT

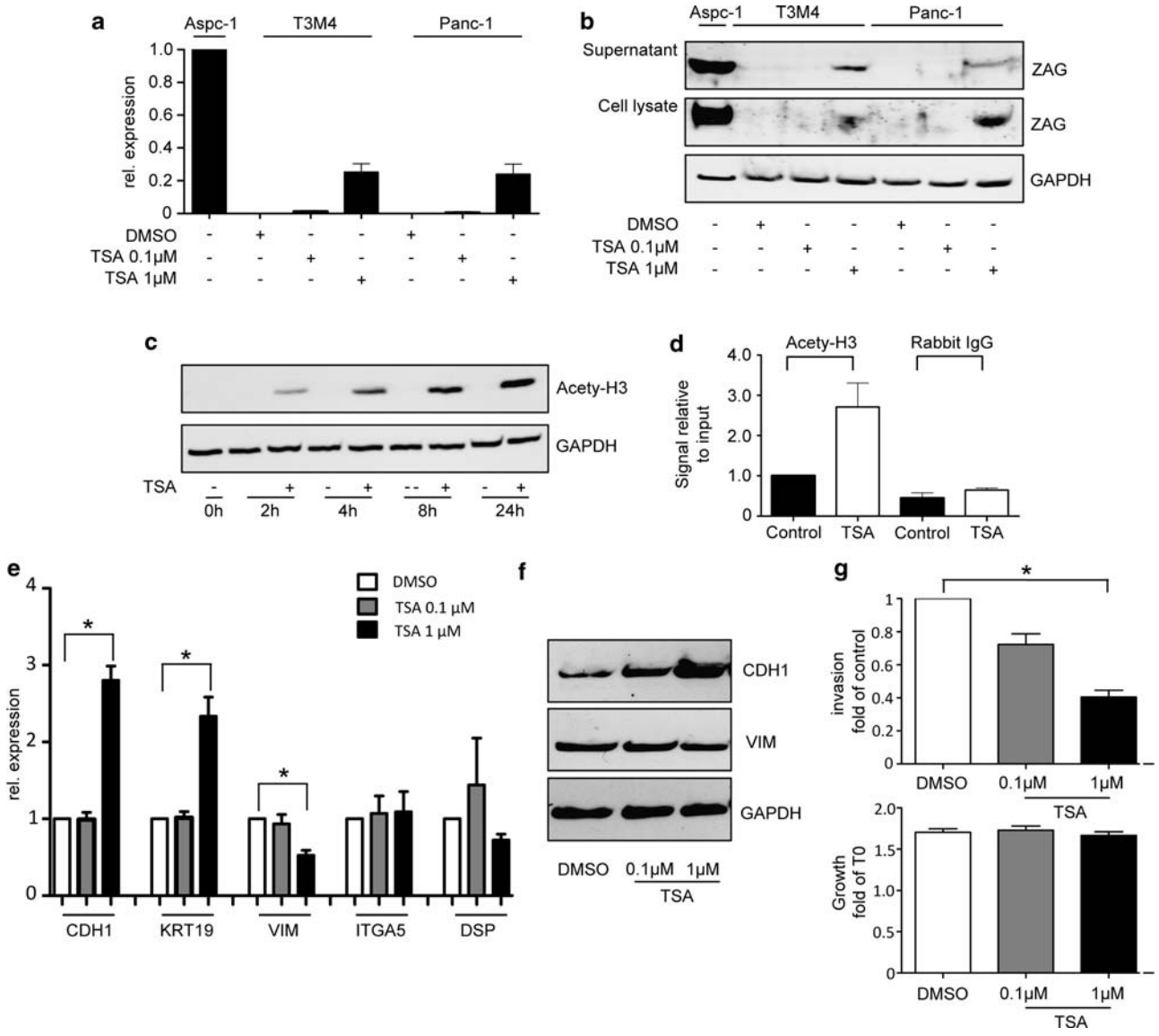

Figure 3 Histone deacetylase inhibition reconstitutes ZAG expression and induces MET in pancreatic cancer cells. (**a**) TSA treatment reconstitutes ZAG mRNA expression in ZAG-negative cell lines (Panc-1 and T3M4). QRT–PCR assays were repeated three times and data are shown as relative expression (normalized to Aspc-1 levels). (**b**) Correspondingly, ZAG protein is found in both supernatants and cell lysates of Panc-1 and T3M4 cells after TSA treatment (immunoblot analysis). One representative immunoblot out of the three independent experiments is shown. (**c**) TSA treatment induces a time-dependent histone H3 acetylation in Panc-1 cells. One representative immunoblot out of the two independent experiments is shown. (**d**) Binding of acetylated histone H3 to the ZAG promoter (Panc-1 cells) is significantly increased following a 2 h TSA treatment (white bars, compared with control, black bars). (**e**) TSA treatment in Panc-1 cells induces an MET program as documented by the increased expression of epithelial markers with a concomitant decreased expression of mesenchymal markers (QRT–PCR; CDH1: E-cadherin, KRT19: keratin 19, VIM: vimentin, ITGA5: integrin-α5, DSP: desmoplakin, $*P<0.05$; relative expression fold of control). (**f**) Changes in CDH1 and VIM levels are confirmed by immunoblot analysis. (**g**) In a Matrigel invasion assay, TSA treatment significantly decreases Panc-1 cell invasiveness (upper panel), whereas no effect on cell proliferation (lower panel) is seen. Values shown are the mean ± s.e.m., fold of control (DMSO) obtained from three independent experiments, $*P<0.05$.

might be attributed to a (direct/indirect) blockade of endogenous TGF-β signaling. Furthermore, it has recently been shown that in Smad4-deficient pancreatic cancer cell lines, autocrine activation of the TGF-β receptor system occurs (Subramanian *et al*., 2004). As Aspc-1 cells are Smad4 negative due to a point mutation (Wan *et al*., 2005), we selectively inhibited type I TGF-β receptor/ALK5 (SB525354) and both type I and type II TGF-β receptors (LY364847) after having silenced ZAG. Though ALK5/type I TGF-β receptor blockade by SB525354 had no effect, the combined inhibition of type I and type II TGF-β receptors by LY364847 reversed the morphological changes elicited by ZAG silencing (Figure 4c, left panel). Furthermore, LY364847 treatment alone induced upregulation of CDH1 confirming an important role of endogenous TGF-β in

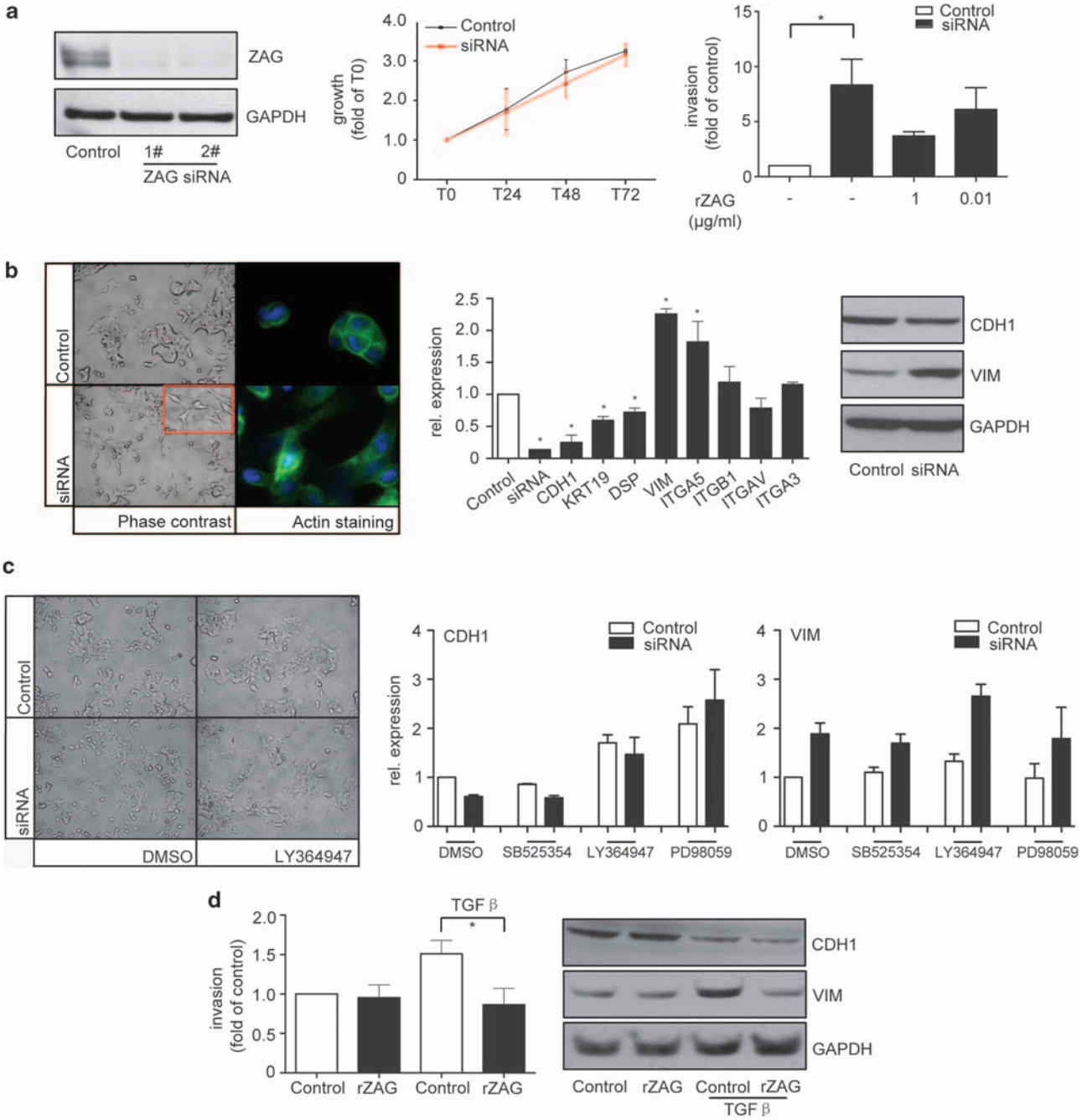

Figure 4 ZAG inhibits invasion of pancreatic cancer cells by blocking TGF-β-mediated EMT. (**a**) ZAG silencing with two sets (1# and 2#) of specific siRNA or negative control siRNA (control) at 48 h (left panel). Proliferation of Aspc-1 cells as assessed by 3-(4,5-dimethylthiazole-2-yl) 2,5-diphenyltetrazolium bromide assays following ZAG siRNA: ZAG siRNA does not change the proliferation rates (middle panels). Data from three independent experiments are expressed as mean ± s.e.m. In a Matrigel invasion assay, ZAG silencing strikingly increases Aspc-1 cancer cell invasiveness, which is partially reversible by pre-incubation with rZAG (right panel). Values shown are the mean ± s.e.m. fold of negative control (control) obtained from three independent experiments, $*P<0.05$. (**b**) ZAG RNAi in Aspc-1 induces fibroblast-like changes in cellular morphology (left panel, phase contrast and actin labeling). The morphological changes were accompanied by the decreased expression of epithelial markers with a concomitant increased expression of mesenchymal markers (QRT–PCR, middle panel; CDH1: E-cadherin, KRT19: keratin 19, DSP: desmoplakin, VIM: vimentin, ITGA5: integrin-α5, ITGB1: integrin-β 1, ITGAV: integrin-αV, ITGA3: integrin-α3, $*P<0.05$; relative expression fold of control). Changes in CDH1 and VIM levels are confirmed by immunoblot analysis (right panel). (**c**) Blockade of endogenous TGF-β signaling by LY 364947 reverses the morphological changes elicited by ZAG silencing in Aspc-1 cells (left panel, phase contrast). Treatment with LY 364947 and PD 98059 increases expression of CDH1 and reverts downregulation of CDH1 induced by ZAG RNAi (QRT–PCR, middle panel). No effects on VIM expression are seen (right panel, relative expression fold of control in DMSO treated group), SB 525354 has no effect on either the expression of CDH1 or VIM. (**d**) *In vitro* cell invasion assay: rZAG reverts TGF-β-induced invasion of Panc-1 cancer cells (left panel). Expression of CDH1 and VIM after 48 h of incubation with TGF-β1 (with or without rZAG); loading control: GAPDH. One representative immunoblot out of three independent experiments is shown.

EMT/MET; although LY 364847 had no influence on basal or induced expression of VIM by ZAG silencing (Figure 4c, right panel), it totally abolished the down-regulation of CDH1 after ZAG RNAi (Figure 4c, middle panel). In addition, inhibition of ERK signaling using an inhibitor of mitogen-activated protein kinase kinase (MEK, PD-98059) induced a similar effect as LY364847 (Figure 4c, middle and right panel). These data suggest that both TGF-β and ERK signaling are involved in EMT mediated by the loss of ZAG. To corroborate these findings, we used the highly invasive pancreatic cancer cell line Panc-1, which also possesses an intact TGF-β signaling pathway but does not express ZAG, for further analyses. Consistent with the recently reported data (Ellenrieder *et al*., 2001), invasion assays revealed that exogenous TGF-β1 increased invasiveness of Panc-1 cells. Though rZAG alone had no effect on invasiveness, it strongly attenuated TGF-β1-mediated tumor cell invasion and VIM upregulation (Figure 4d). It is interesting that in comparison with the TGF-β receptor blocking experiments, ZAG did not change TGF-β-induced CDH1 suppression (Figure 4d, right panel).

ZAG induces mesenchymal-to-epithelial transdifferentiation by modulating TGF-β-mediated ERK signaling

Both Panc-1 and Aspc-1 cells carry a constitutively active K-Ras mutation. As it has been shown that constitutive activation of Ras is required for TGF-β-induced EMT in Panc-1 cells (Ellenrieder *et al*., 2001; Horiguchi *et al*., 2009), we analyzed whether ZAG was involved in the interaction between Ras/ERK and TGF-β signaling. To rule out the possibility that ZAG might have a direct effect on the transduction of the TGF-β signal, we examined the phosphorylation of Smad2 following treatment with exogenous TGF-β1 (with or without incubation with rZAG) in Panc-1 cells. Although TGF-β1 time-dependently induced phosphorylation of Smad2, neither rZAG alone nor rZAG in combination with TGF-β1 had any additional effect (Figure 5a). As exogenous TGF-β1 causes sustained phosphorylation of ERK2, which is essential for TGF-β1-mediated EMT (Ellenrieder *et al*., 2001), we evaluated ERK2 phosphorylation following treatment with TGF-β1 for 24 h (± rZAG). These assays revealed that the TGF-β1-mediated increase in ERK2 phosphorylation was blocked by preincubation with rZAG (Figure 5b). Because TGF-β1-mediated inhibition of cell growth is partially transduced by transcriptional induction of the cell-cycle inhibitor p21(WAF1/Cip1; p21), regulated by Smad4 (Finkel, 1996), we used p21 as an internal control for the activation of the Smad4-dependent TGF-β pathway. These experiments revealed that in Panc-1 cells with intact Smad4, TGF-β1 treatment induced expression of p21 that remained unchanged by treatment with rZAG (Figure 5b), suggesting that rather the cross talk between TGF-β and Ras/ERK signaling than the Smad4-dependent pathway is blocked by rZAG. Accordingly, in Aspc-1 (Smad4-negative) cells, ZAG silencing, as well as TGF-β1 treatment, caused sustained phosphorylation of ERK2, presumably due to (facilitation of) activation of endogenous TGF-β signaling (Figure 5c). Interestingly, ZAG RNAi alone or in combination with TGF-β1 induced p21 expression (Figure 5c).

ZAG at the crossroads of cellular differentiation and energy control

To further characterize signal transduction pathways modulated by ZAG, we used an RT–PCR-based

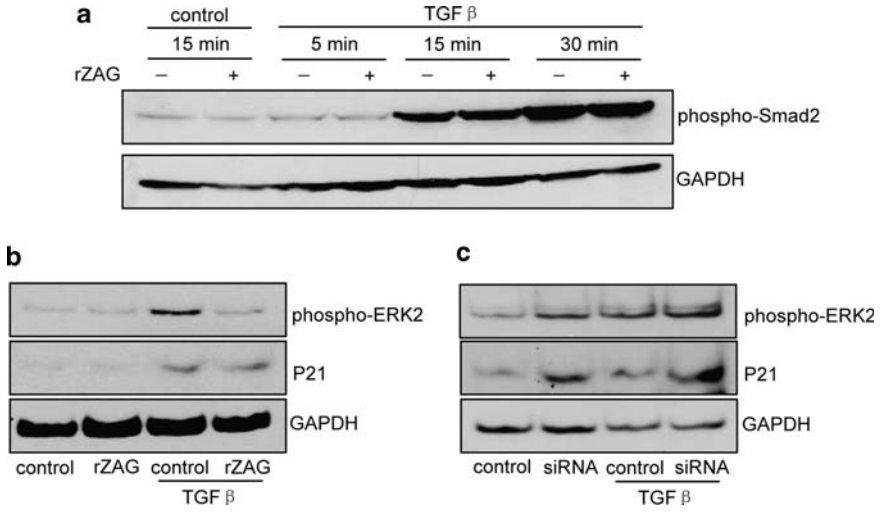

Figure 5 ZAG exerts MET effects by modulating TGF-β-mediated ERK signaling. (**a**) Time-dependent, increasing phosphorylation of Smad2 following TGF-β treatment with or without rZAG. Loading control: GAPDH. (**b**) Increased phospho-ERK2 following incubation with TGF-β1 is reverted by pre-treatment with rZAG; p21 levels are unaltered (Panc-1 cells). One representative immunoblot out of three independent experiments is shown. (**c**) ZAG silencing increases phosphorylation of ERK2 and p21 levels, which is further enhanced following incubation with TGF-β1. One representative immunoblot out of three independent experiments is shown.

pathway array to compare expression changes of a large number of genes after ZAG silencing in Aspc-1 cells (Figure 6a). In line with our findings above, BMP4 and CDKN1B were increased, which reflected the activation of endogenous TGF-β signaling (Lecanda *et al*., 2009). In particular, exogenous human recombinant BMP4 (rBMP4) treatment induced an EMT program in Panc-1 and Su86.86 cells (Supplementary Figures 5A and B), which is consistent with published results (Ellenrieder *et al*., 2001; Hamada *et al*., 2007). Furthermore, *BCL2L1*, *CCND1* and *MYC*, which are survival pathway-related genes, were upregulated underscoring the importance of prosurvival signals during EMT (Biliran *et al*., 2005; Freemantle *et al*., 2007; Barbie *et al*., 2009). EGR1, which represents a mitogenic pathway, was downregulated, consistent with the observed increased expression of the cell-cycle inhibitor p21 (Lim *et al*., 2008). Surprisingly, HK2 and CEBPB, which are insulin-responsive factors, were highly induced after ZAG RNAi. We thus speculate that the increased levels of HK2, which catalyzes one of the first steps in glucose metabolism, reflect an increased demand for glucose

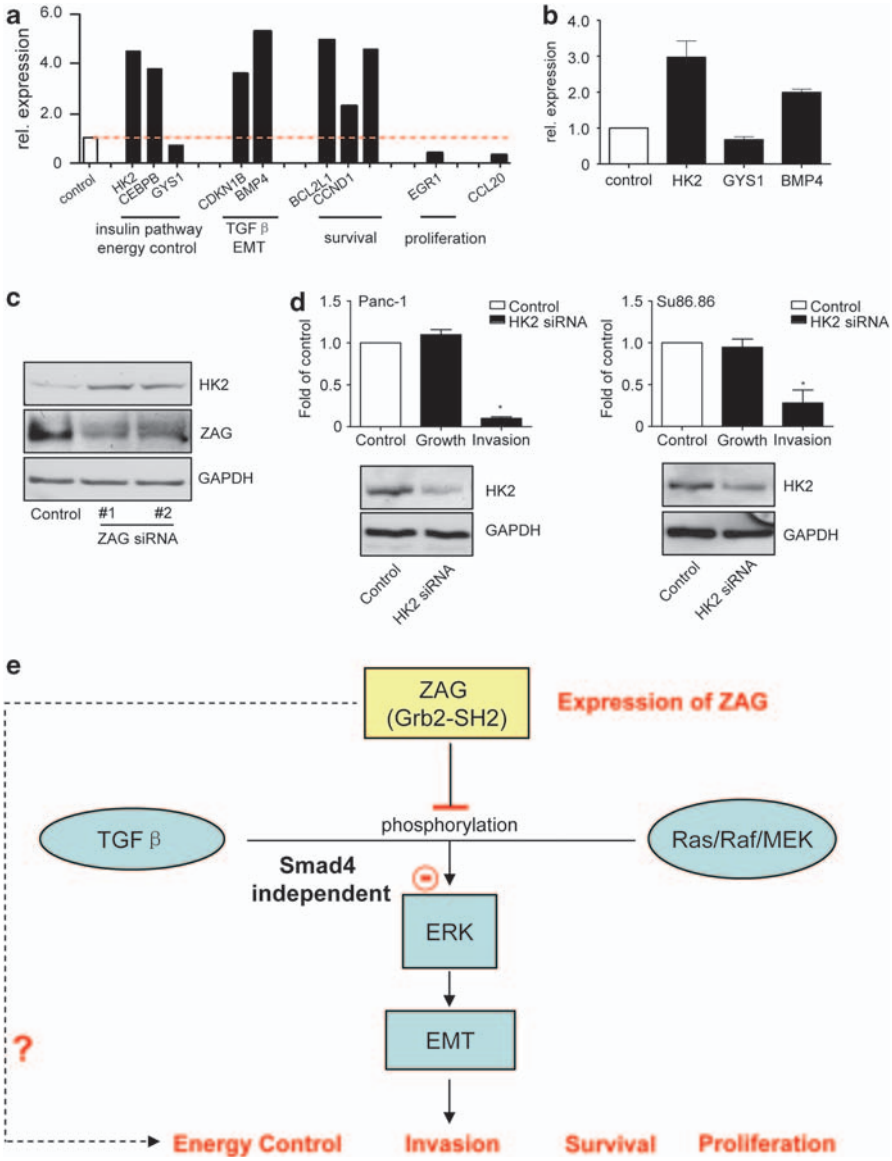

Figure 6 ZAG at the crossroads of cellular differentiation and energy control. (**a**) Results of the real-time PCR pathway finder array following ZAG RNAi. Increased expression of CEBPB and HK2 (insulin-responsive factors) with the downregulation of GYS1 indicates a shift towards a high-glucose metabolic rate. Increased expression of CDKN1B and BMP4 reflects activation of endogenous TGF-β signaling. In addition, changes in BCL2L1, CCND1, MYC and EGR1 suggest an increased prosurvival signal. (**b**) QRT–PCR was performed to confirm expression changes of HK2, GYS1 and BMP4 after ZAG RNAi in Aspc-1 cells; relative expression fold of control (mean ± s.e.m.) obtained from three independent experiments. (**c**) The changes in HK2 are confirmed by immunoblot analysis. (**d**) HK2 silencing with specific siRNA or negative control siRNA (control) at 72 h in Panc-1 and Su86.86 cells (lower panel). In a Matrigel invasion assay, HK2 silencing strikingly decreases Panc-1 and Su86.86 cancer cell invasiveness, whereas no influence on cell proliferation is observed (upper panel). Values shown are the mean ± s.e.m., fold of negative control (control) obtained from three independent experiments, $*P<0.05$. (**e**) Schematic interference model: ZAG modulates TGF-β and Ras/ERK signaling.

(and thus an increased energy need) when cancer cells undergo EMT. Correspondingly, GYS1—an enzyme responsible for adding glucose monomers to glycogen—was downregulated. These results were confirmed by independent QRT–PCR assays (Figure 6b), and increased expression of HK2 was confirmed on the protein level (Figure 6c). To interrogate whether HK2 is functionally relevant for EMT and cell invasion, we chose the highly invasive pancreatic cancer cell lines Panc-1 and Su86.86 for further analysis. As expected, HK2 RNAi suppressed HK2 expression in Panc-1 and Su86.86 cells (Figure 6d, lower panel). Though downregulation of HK2 did not significantly affect cell proliferation, it strikingly inhibited cell invasion (Figure 6d, upper panel; confirmed using another HK2 siRNA; data not shown). However, no changes in the expression of EMT markers after silencing HK2 were observed in Panc-1 and Su86.86 cells (data not shown). These results suggest that a certain level of HK2 or glucose metabolism is essential for maintaining the basal invasiveness of cancer cells rather than their differentiation status. Therefore, we speculate that these molecules cooperatively promote EMT and cell invasion following a loss of ZAG. To conclude, loss of ZAG in Aspc-1 seems not only to induce EMT but to also reprogram the cells within a series of concerted cellular events consisting of increased energy consumption, a prosurvival signal and a lower proliferation rate (Figure 6e).

Discussion

In K-ras-transformed pancreatic cancer cells, epithelial plasticity and EMT are increasingly seen as epigenetic phenomena (Singh *et al*., 2009), which is supported by recent findings in other malignancies, such as breast cancer in which a signal from the tumor microenvironment (for example, TGF-β) can induce phenotypic and gene expression changes associated with *de novo* epigenetic events important for EMT (Dumont *et al*., 2008). In general, methylation (regulated by DNA methyltransferases and histone deacetylation (regulated by HDACs) are two main mechanisms through which epigenetic regulation is conferred (Jaenisch and Bird, 2003; Glozak and Seto, 2007). By removing acetyl groups from histones, it is found that HDACs create a non-accessible chromatin conformation that reduces the transcription of genes (that is, those which are implicated in the control of cell growth differentiation and apoptosis) (Glozak and Seto, 2007). In PDAC, HDAC inhibitors have been shown to block cell proliferation to promote differentiation and to induce apoptosis (Fritsche *et al*., 2009; Von Burstin *et al*., 2009); we showed that TSA blocks cell invasion and promotes mesenchymal-to-epithelial transdifferentiation (MET) in human PDAC cells, therefore, these might constitute promising anticancer agents—given that gene-specific control would be possible. The link between the epigenetic HDAC machinery, EMT and metastasis has also recently been shown using highly metastatic (mesenchymal phenotype) cancer cells derived from a genetically engineered mouse pancreas cancer model; in these cells, silencing of CDH1 was mediated by a transcriptional repressor complex containing snail, HDAC1 and HDAC2 (von Burstin *et al*., 2009). In our study, we now show that the expression of ZAG—an EMT related gene—is also lost due to histone deacetylation. However, because validated siRNA transfection against HDAC1-7 failed to significantly reconstitute ZAG expression in Panc-1 cells (data not shown), we hypothesize that a so far unknown co-repressor or repressor complex exists. Using a set of *in vitro* experiments, we showed that ZAG specifically blocks signaling between TGF-β and Ras/ERK. Overexpression of TGF-β ligands and their receptors as well as activating mutations of K-Ras occurs at a very high frequency in PDAC and interactions of these two major pathways have been shown to be crucial in pancreatic carcinogenesis (Lemoine *et al*., 1992; Friess *et al*., 1993). In addition, the Ras/ERK cascade has been shown to be activated by members of the TGF-β family contributing to TGF-β-mediated effects, such as EMT (Ellenrieder *et al*., 2001; Horiguchi *et al*., 2009). The TGF-β signal transducers Smad2 and Smad3 have also been shown to be phosphorylated by ERK (de Caestecker *et al*., 1998; Kretzschmar *et al*., 1999). Recent studies revealed that ERK2 phosphorylation through TGF-β, which occurs in a Ras-dependent way, is essential for TGF-β-mediated EMT (Ellenrieder *et al*., 2001; Horiguchi *et al*., 2009). At the same time, it is important to consider that activating K-Ras mutations in the pancreatic cancer cells do not result in constitutively increased ERK signaling (Giehl *et al*., 2000). Interestingly, in a mouse colorectal cancer model, the K-Ras tumor phenotype was associated with an attenuated signaling through the mitogen-activated protein kinase pathway (Haigis *et al*., 2008). Thus, it is still not clear whether, due to relatively 'low' levels of basal Ras/ERK activity, the threshold of activation of this pathway (that is, by TGF-β) is also relatively low. In our study, we showed that TGF-β1-mediated ERK2 phosphorylation was blocked by ZAG and that this effect was associated with EMT and an increased invasive potential of two pancreatic cancer cell lines, which carry the constitutively active Ras mutation. ZAG seems to function like a specific barrier that interrupts TGF-β/ERK signaling. We further identified (http://scansite.mit.edu) the growth factor receptor-binding protein, 2-Src homology 2 (Grb2–SH2, TLKDIVEYYNDSNGS) domain, within the ZAG sequence. The Grb2–SH2 domain has been described as docking site for activated receptors and, therefore, is important in the oncogenic Ras signal transduction pathway (Lung and Tsai, 2003; Benfield *et al*., 2007). We thus speculate that ZAG might exert its effect on TGF-β and Ras/ERK signaling through the Grb2–SH2 domain. However, a synthesized small peptide including this region failed to reconstitute the function of the full-length protein in our experimental setup (data not shown), adding another layer of complexity to the underlying mechanism. Nevertheless,

the exact molecular mechanisms deserve (and require) further investigation.

Though obesity and insulin resistance are potential risk factors for developing pancreatic cancer (Michaud *et al*., 2001; Calle *et al*., 2003), the underlying molecular mechanisms remain elusive. A recent study revealed that high-fat-diet-induced obesity in mice accelerated the development of PanIN in the context of embryonic K-Ras activation through changes in energy metabolism. These data suggested changes in energy metabolism rather than insulin resistance as key elements in early carcinogenesis of PDAC (Khasawneh *et al*., 2009). Recent evidence has also established a link between low serum levels of ZAG and obesity in humans; however, whether ZAG serum levels are also related to insulin resistance is still under debate (Marrades *et al*., 2008). Nonetheless, the antidiabetic properties of human ZAG have recently been shown in type 2 diabetes in the ob/ob mouse model (Russell and Tisdale, 2010). Furthermore, ZAG-deficient animals fed by a standard or a lipid-rich diet were heavier than wild-type mice (Rolli *et al*., 2007). Therefore, we hypothesized that ZAG might be involved in early carcinogenetic events in the pancreas through a modulation of energy metabolism pathways. In line with this assumption, silencing of ZAG in PDAC cells lines upregulated the two insulin responsive-factors HK2 and CEBPB, whereas GYS1 levels were decreased. These data suggest that the cancer cells are 'pushed' toward a high-glucose metabolic state that seems to be important for cell invasion. Correspondingly, silencing of HK2 in highly invasive cancer cells strikingly attenuated their invasiveness, which further underscores an essential role of energy metabolism in cellular invasion events. Moreover, such a shift in energy metabolism occurs distinctively within EMT. Though our study is limited by *in vitro* tissue culture conditions with supraphysiological levels of glucose, oxygen and growth factors, it seems possible that ZAG might serve as a critical mediator adjusting energy metabolism according to the differentiation status of cancer cells. Because cancer cells consume glucose at an accelerated rate with reduced oxidative phosphorylation even in the presence of oxygen (known as the 'Warburg effect'), such a capacity confers a distinct competitive advantage compared with normal epithelial cells (Mathupala *et al*., 2006; Christofk *et al*., 2008). As a consequence, cancer cells that have undergone EMT—inducing a high-glucose metabolic rate—may have gained further malignant 'advantages' compared with the more epithelial, earlier cancer cell stages. Such advantages may help these cells to migrate or survive under even more unfavorable conditions, that is, in 'new' microenvironments as present after having metastasized to distant organs.

In conclusion, our data provide evidence that ZAG affects the differentiation status of pancreatic cancer by blocking the cross talk between TGF-β and Ras/ERK signaling. EMT elicited by loss of ZAG is accompanied by a series of concerted cellular events including a shift in energy metabolism, prosurvival signals and reduced cell proliferation. We speculate that targeting this cross talk by restoring the function of ZAG might constitute a new rational approach to reduce/reverse EMT in pancreatic cancer.

Materials and methods

Patients and tissue sampling

Tissue sampling and processing was performed as previously described (Zhang *et al*., 2007). Histological examination was carried out by an experienced pathologist (IE). The use of tissue for this study was approved by the local ethics committees and written informed consent was obtained from the patients before the operation.

Cell culture

Seven pancreatic cancer cell lines—ASPC1, Capan1, Colo357, MiaPaca2, SU86.86, Panc1 and T3M4—were cultured was previously described (Zhang *et al*., 2007). PET cell lines were cultured in Dulbecco's modified Eagle's medium (Bon-1 and QGP-1) or RPMI 1640 (CM) cell culture media supplemented with 10% fetal bovine serum, 100 U/ml penicillin and 100 μg/ml streptomycin at 37 °C, 5% CO_2. The inhibitor of methylation, 5-aza (5 μM; Sigma-Aldrich, St Louis, MO, USA), and the inhibitor of HDAC, TSA (0.1 and 1 μM; Sigma-Aldrich), were added to proliferating or confluent cells (Panc-1, T3M4, Colo-357 and Su86.86) for 72 and 24 h. Cells were then lysed and processed for total RNA extraction or whole cellular extract preparation as described thereafter. For functional assays, cells were treated with TSA for 72 h, and were then subjected to invasion and proliferation assays in the absence of TSA. For the human recombinant BMP4 (rBMP4) assays, Panc-1 and Su86.86 cells were treated with rBMP4 (100 ng/ml; catalog no. 314-BP/CF; R&D, Wiesbaden-Nordenstadt, Wiesbaden, Germany) in serum-free medium for 6 consecutive days before the extraction of protein.

QRT–PCR

The mRNA extraction, cDNA synthesis and QRT–PCR were performed as described previously (specimens used: normal $n=19$; PDAC $n=57$) (Michalski *et al*., 2007a). Data are presented as relative expression fold. β-Actin and hypoxanthine phosphoribosyltransferase 1 were used as housekeeping genes. Sequences of primers are provided in Supplementary data section.

Immunohistochemistry

Immunohistochemistry was performed using the Dako Envision System (Dako Cytomation GmbH, Hamburg, Germany) as previously described (Michalski *et al*., 2007b). In brief, tissue sections or a PanIN array (Esposito *et al*., 2007) were incubated with rabbit anti-human ZAG polyclonal antibodies (1:500, catalog no. RD181093100; BioVendor, Heidelberg, Germany) at 4 °C overnight followed by incubation with a horseradish-peroxidase-linked goat anti-rabbit antibody (Dako Cytomation GmbH), followed by a reaction with diaminobenzidine and counterstaining with Mayer's hematoxylin. To confirm antibody specificity, we incubated tissue sections in the absence of the primary antibodies with negative control rabbit or mouse IgG. Under these conditions, no immunostaining was detected.

Immunofluorescence

Immunofluorescence was performed as previously described (Michalski *et al*., 2008). In brief, cytoskeleton actin was labeled

with Alexa Fluor 488 phalloidin (Molecular Probes, Eugene, OR, USA). The sections were subsequently mounted with DAPI and antifading medium (Gel/mount; Abcam, Cambridge, UK).

Serum collection and enzyme-linked immunosorbent assay
The serum collection and enzyme-linked immunosorbent assay were performed as previously described (Zhang *et al*., 2007). The study was approved by the ethics committee of the University of Heidelberg and written informed consent was obtained from all individuals from whom serum samples were collected. In brief, rabbit anti-ZAG antibody (0.05 μg/ml, catalog no. sc-11358; Santa Cruz Biotechnology, Santa-Cruz, CA, USA) was used as the capture antibody and mouse anti-ZAG antibody (1 μg/ml, catalog no. sc-13585; Santa Cruz Biotechnology) was used as the detection antibody.

Immunoblot analysis
Cultured pancreatic cancer cells were lysed in ice-cold RIPA buffer (catalog no. 9806; Cell Signaling, Danvers, MA, USA) containing one tablet EDTA-free protease inhibitor cocktail (Roche Diagnostics, Mannheim, Germany) for 10 min. For the detection of phospho-p44/42 and phospho-Smad2, we used a cell lysis buffer (catalog no. 9803; Cell Signaling). The western blot analysis was performed as previously described (Ketterer *et al*., 2009). The following antibodies were used: mouse anti-ZAG (catalog no. sc-13585, 1:500; Santa Cruz Biotechnology), rabbit anti-phospho-p44/42 mitogen-activated protein kinase (Erk1/2) (Thr202/Tyr204; 1:1000, catalog no. 9101; Cell Signaling), rabbit anti-p21Waf1/Cip1 (12D1; 1:1000, catalog no. 2947; Cell Signaling), rabbit anti-phospho-Smad2 (Ser465/467;138D4; 1:1000, catalog no. 3108; Cell Signaling), rabbit anti-CDH1 (24E10; 1:5000, catalog no. 3195; Cell Signaling), mouse anti-VIM (SKU catalog no. 18-0052, 1:15000; Invitrogen, Carlsland, CA, USA), rabbit anti-HK2 (C64G5, 1:2000, catalog no. 2867; Cell signaling) or rabbit anti-GAPDH (1:5000; Santa Cruz Biotechnology) overnight at 4 °C.

Chromatin immunoprecipitation assay
Chromatin immunoprecipitations were performed using the Magna ChIP A Chromatin Immunoprecipitation Kit (catalog no. 17-610; Millipore, Temecula, CA, USA) according to the manufacturer's instructions. Equal amounts of cross-linked chromatin from 1×10^6 Panc-1 cells treated with TSA (1 μM) or DMSO for 2 h were precipitated with either 10 μl acetylated-H3 antibody or 10 μl normal rabbit IgG overnight. The total chromatin (1%) in each reaction was saved as an 'input' for later quantification. After purification, the enriched DNA was quantified by RT–PCR using primers specific for the ZAG promoter. The amount of immunoprecipitated DNA in each sample is represented as signal relative to input chromatin. Each yielded value was then normalized to control (DMSO treated). The assays were repeated three times. Sequences of primers are provided in Supplementary data section.

siRNA transfections
Synthetic siRNA oligonucleotides for ZAG and negative control siRNA were purchased from Ambion (#s1848_1# and s1849_2#; Applied Biosystems, Darmstadt, Germany) and were prepared and stored according to the manufacturer's instructions. siRNA transfections were carried out according to the manufacturer's instructions. siPORT NeoFX Transfection Agent (Ambion Applied Biosystem, Austin, TX, USA) transfection reagent was used. The final concentration of both the control and specific oligonucleotides was 40 nM. The efficacy of the siRNA transfection was ascertained by immunoblot analysis after 48 h of transfection. Synthetic siRNA oligonucleotides for HK2 were obtained from Qiagen (catalog nos SI03021935_1# and SI00287329_2#, Qiagen, Hilden, Germany) and transfected with HiPerFect transfection reagent according to the manufacturer's instructions. The efficacy of HK2 downregulation was assessed after 72 h of transfection. The sequences of siRNA oligonucleotides are provided in Supplementary data section.

Proliferation assays
Cell growth was determined using the 3-(4,5-dimethylthiazole-2-yl)2,5-diphenyltetrazolium bromide (5 mg/ml in phosphate-buffered saline; Sigma-Aldrich) colorimetric growth assay as previously described (Zhang *et al*., 2007). All assays were performed in triplicates and were repeated three times.

Invasion assays
To assess cell invasion *in vitro*, we used 24-well Matrigel invasion chambers with 8-mm pore sizes (BD Biosciences, San Jose, CA, USA) and reconstituted them with 600 μl serum-free Dulbecco's modified Eagle's medium in both the top and the bottom chambers for 2–4 h. Cells were trypsinized and were seeded into the top chamber at a density of 5×10^4 cells (Aspc-1) or 1.25×10^4 cells (Panc-1 and Su86.86) per well in 500 μl Dulbecco's modified Eagle's medium containing 0.5% fetal calf serum. The outer chambers contained 0.7 ml of medium (10% fetal calf serum). According to each experimental setup, TGF-β (CF111; Millipore) or rZAG was added to the top chambers at a dose of 10 ng/ml, 1 or 0.01 μg/ml. After incubation at 37 °C for 24 h, cells remaining attached to the upper surface of the membrane were carefully removed with cotton swabs, whereas cells that reached the underside of the chamber were stained with hematoxylin and eosin and were counted. All experiments were repeated three times.

Detection of EMT markers, phospho-ERK and p21
To analyze the effect of TGF-β and rZAG on EMT, we grew Panc-1 cells to 70% confluence in Dulbecco's modified Eagle's medium containing 10% fetal calf serum. Cells were washed twice in serum-free medium and were starved for 24 h in serum-free medium, and were finally treated for 48 h with TGF-β (10 ng/ml) or carrier protein. rZAG was added at a concentration of 1 μg/ml, 90 min before the application of TGF-β. For Aspc-1, cells were (siRNA) transfected as described. At 24 h after transfection, the medium was removed and the cells were washed twice in serum-free medium and were starved for 12 h in serum-free medium. The cells were then treated for 36 h with TGF-β (10 ng/ml) or carrier protein. For the endogenous TGF-β signaling blocking assay, SB525354 (200 nM), LY-364947 (25 μM) and PD98059 (50 μM, all from Tocris Bioscience, Bristol, UK) were used to treat Aspc-1 cells for 24 h in serum-free medium before RNA extraction. For the detection of phospho-ERK and p21, a similar experimental setup was carried out with the exception that TGF-β treatment was restricted to 24 h. All experiments were repeated three times.

RT–PCR pathway finder array
All the reagents and materials for the PCR array (PAHS-014) were purchased from SABiosciences (Frederick, MD, USA). The assay was performed according to the manufacturer's instruction. Data were analyzed using the web-based

software from SABiosciences (http://www.sabiosciences.com/pcr/arrayanalysis.php).

Statistical analysis

For statistical analyses, the GraphPad Prism 5 Software (GraphPad, San Diego, CA, USA) was used. The χ^2-test was used to compare the numbers of ZAG-positive samples between PanIN lesions, primary and metastatic PDAC, as well as the frequency of ZAG-positive samples in PETs, primary PDAC and ACCs. Unless otherwise stated, an unpaired *t*-test was used for group-wise comparisons. The level of statistical significance was set at $P<0.05$. Results are expressed as mean ± standard error of the mean (s.e.m.) unless indicated otherwise.

Conflict of interest

The authors declare no conflict of interest.

Acknowledgements

We thank Felicitas Altmayr, Tanja Rossmann-Bloeck, Manja Thorwirth and Carmen Marthen for excellent technical support. This study was in part supported by the European Union (within the framework of the 'MolDiagPaca' project; to JK, CWM and HF) and by the commission for clinical research of the TU Munich (KKF). BK received a fellowship from the Scholarship Council of the Ministry of Education of China.

References

Barbie DA, Tamayo P, Boehm JS, Kim SY, Moody SE, Dunn IF *et al*. (2009). Systematic RNA interference reveals that oncogenic KRAS-driven cancers require TBK1. *Nature* **462**: 108–112.

Benfield AP, Whiddon BB, Clements JH, Martin SF. (2007). Structural and energetic aspects of Grb2-SH2 domain-swapping. *Arch Biochem Biophys* **462**: 47–53.

Biliran Jr H, Wang Y, Banerjee S, Xu H, Heng H, Thakur A *et al*. (2005). Overexpression of cyclin D1 promotes tumor cell growth and confers resistance to cisplatin-mediated apoptosis in an elastase-myc transgene-expressing pancreatic tumor cell line. *Clin Cancer Res* **11**: 6075–6086.

Bing C, Bao Y, Jenkins J, Sanders P, Manieri M, Cinti S *et al*. (2004). Zinc-alpha2-glycoprotein, a lipid mobilizing factor, is expressed in adipocytes and is up-regulated in mice with cancer cachexia. *Proc Natl Acad Sci USA* **101**: 2500–2505.

Brabletz T, Jung A, Spaderna S, Hlubek F, Kirchner T. (2005). Opinion: migrating cancer stem cells—an integrated concept of malignant tumour progression. *Nat Rev Cancer* **5**: 744–749.

Burgi W, Schmid K. (1961). Preparation and properties of Zn-alpha 2-glycoprotein of normal human plasma. *J Biol Chem* **236**: 1066–1074.

Calle EE, Rodriguez C, Walker-Thurmond K, Thun MJ. (2003). Overweight, obesity, and mortality from cancer in a prospectively studied cohort of U.S. adults. *N Engl J Med* **348**: 1625–1638.

Christofk HR, Vander Heiden MG, Harris MH, Ramanathan A, Gerszten RE, Wei R *et al*. (2008). The M2 splice isoform of pyruvate kinase is important for cancer metabolism and tumour growth. *Nature* **452**: 230–233.

De Caestecker MP, Parks WT, Frank CJ, Castagnino P, Bottaro DP, Roberts AB *et al*. (1998). Smad2 transduces common signals from receptor serine-threonine and tyrosine kinases. *Genes Dev* **12**: 1587–1592.

Dembinski JL, Krauss S. (2009). Characterization and functional analysis of a slow cycling stem cell-like subpopulation in pancreas adenocarcinoma. *Clin Exp Metastasis* **26**: 611–623.

Diez-Itza I, Sanchez LM, Allende MT, Vizoso F, Ruibal A, Lopez-Otin C. (1993). Zn-alpha 2-glycoprotein levels in breast cancer cytosols and correlation with clinical, histological and biochemical parameters. *Eur J Cancer* **29A**: 1256–1260.

Dumont N, Wilson MB, Crawford YG, Reynolds PA, Sigaroudinia M, Tlsty TD. (2008). Sustained induction of epithelial to mesenchymal transition activates DNA methylation of genes silenced in basal-like breast cancers. *Proc Natl Acad Sci USA* **105**: 14867–14872.

Ellenrieder V, Hendler SF, Boeck W, Seufferlein T, Menke A, Ruhland C *et al*. (2001). Transforming growth factor beta1 treatment leads to an epithelial-mesenchymal transdifferentiation of pancreatic cancer cells requiring extracellular signal-regulated kinase 2 activation. *Cancer Res* **61**: 4222–4228.

Esposito I, Kleeff J, Abiatari I, Shi X, Giese N, Bergmann F *et al*. (2007). Overexpression of cellular inhibitor of apoptosis protein 2 is an early event in the progression of pancreatic cancer. *J Clin Pathol* **60**: 885–895.

Evdokimova V, Tognon C, Ng T, Sorensen PH. (2009). Reduced proliferation and enhanced migration: two sides of the same coin? Molecular mechanisms of metastatic progression by YB-1. *Cell Cycle* **8**: 2901–2906.

Finkel E. (1996). High hopes for p21 in cancer treatment. *Lancet* **347**: 1034.

Freemantle SJ, Liu X, Feng Q, Galimberti F, Blumen S, Sekula D *et al*. (2007). Cyclin degradation for cancer therapy and chemoprevention. *J Cell Biochem* **102**: 869–877.

Frenette G, Dube JY, Lazure C, Paradis G, Chretien M, Tremblay RR. (1987). The major 40-kDa glycoprotein in human prostatic fluid is identical to Zn-alpha 2-glycoprotein. *Prostate* **11**: 257–270.

Friess H, Yamanaka Y, Buchler M, Ebert M, Beger HG, Gold LI *et al*. (1993). Enhanced expression of transforming growth factor beta isoforms in pancreatic cancer correlates with decreased survival. *Gastroenterology* **105**: 1846–1856.

Fritsche P, Seidler B, Schuler S, Schnieke A, Gottlicher M, Schmid RM *et al*. (2009). HDAC2 mediates therapeutic resistance of pancreatic cancer cells via the BH3-only protein NOXA. *Gut* **58**: 1399–1409.

Giehl K, Skripczynski B, Mansard A, Menke A, Gierschik P. (2000). Growth factor-dependent activation of the Ras–Raf–MEK–MAPK pathway in the human pancreatic carcinoma cell line PANC-1 carrying activated K-ras: implications for cell proliferation and cell migration. *Oncogene* **19**: 2930–2942.

Glozak MA, Seto E. (2007). Histone deacetylases and cancer. *Oncogene* **26**: 5420–5432.

Haigis KM, Kendall KR, Wang Y, Cheung A, Haigis MC, Glickman JN *et al*. (2008). Differential effects of oncogenic K-Ras and N-Ras on proliferation, differentiation and tumor progression in the colon. *Nat Genet* **40**: 600–608.

Hale LP, Price DT, Sanchez LM, Demark-Wahnefried W, Madden JF. (2001). Zinc alpha-2-glycoprotein is expressed by malignant prostatic epithelium and may serve as a potential serum marker for prostate cancer. *Clin Cancer Res* **7**: 846–853.

Hamada S, Satoh K, Hirota M, Kimura K, Kanno A, Masamune A *et al*. (2007). Bone morphogenetic protein 4 induces epithelial-mesenchymal transition through MSX2 induction on pancreatic cancer cell line. *J Cell Physiol* **213**: 768–774.

Horiguchi K, Shirakihara T, Nakano A, Imamura T, Miyazono K, Saitoh M. (2009). Role of Ras signaling in the induction of snail by transforming growth factor-beta. *J Biol Chem* **284**: 245–253.

Jaenisch R, Bird A. (2003). Epigenetic regulation of gene expression: how the genome integrates intrinsic and environmental signals. *Nat Genet* **33**(Suppl): 245–254.

Jones S, Zhang X, Parsons DW, Lin JC, Leary RJ, Angenendt P *et al*. (2008). Core signaling pathways in human pancreatic cancers revealed by global genomic analyses. *Science* **321**: 1801–1806.

Ketterer K, Kong B, Frank D, Giese NA, Bauer A, Hoheisel J *et al*. (2009). Neuromedin U is overexpressed in pancreatic cancer and increases invasiveness via the hepatocyte growth factor c-Met pathway. *Cancer Lett* **277**: 72–81.

Khasawneh J, Schulz MD, Walch A, Rozman J, Hrabe de Angelis M, Klingenspor M *et al*. (2009). Inflammation and mitochondrial fatty acid beta-oxidation link obesity to early tumor promotion. *Proc Natl Acad Sci USA* **106**: 3354–3359.

Kretzschmar M, Doody J, Timokhina I, Massague J. (1999). A mechanism of repression of TGFbeta/Smad signaling by oncogenic Ras. *Genes Dev* **13**: 804–816.

Lecanda J, Ganapathy V, D'Aquino-Ardalan C, Evans B, Cadacio C, Ayala A *et al*. (2009). TGFbeta prevents proteasomal degradation of the cyclin-dependent kinase inhibitor p27kip1 for cell cycle arrest. *Cell Cycle* **8**: 742–756.

Lemoine NR, Jain S, Hughes CM, Staddon SL, Maillet B, Hall PA *et al*. (1992). Ki-ras oncogene activation in preinvasive pancreatic cancer. *Gastroenterology* **102**: 230–236.

Lim JH, Jung CR, Lee CH, Im DS. (2008). Egr-1 and serum response factor are involved in growth factors- and serum-mediated induction of E2-EPF UCP expression that regulates the VHL-HIF pathway. *J Cell Biochem* **105**: 1117–1127.

Longnecker DS, Terhune PG. (1998). What is the true rate of K-ras mutation in carcinoma of the pancreas? *Pancreas* **17**: 323–324.

Lung FD, Tsai JY. (2003). Grb2 SH2 domain-binding peptide analogs as potential anticancer agents. *Biopolymers* **71**: 132–140.

Marrades MP, Martinez JA, Moreno-Aliaga MJ. (2008). ZAG, a lipid mobilizing adipokine, is downregulated in human obesity. *J Physiol Biochem* **64**: 61–66.

Mathupala SP, Ko YH, Pedersen PL. (2006). Hexokinase II: cancer's double-edged sword acting as both facilitator and gatekeeper of malignancy when bound to mitochondria. *Oncogene* **25**: 4777–4786.

Michalski CW, Laukert T, Sauliunaite D, Pacher P, Bergmann F, Agarwal N *et al*. (2007a). Cannabinoids ameliorate pain and reduce disease pathology in cerulein-induced acute pancreatitis. *Gastroenterology* **132**: 1968–1978.

Michalski CW, Maier M, Erkan M, Sauliunaite D, Bergmann F, Pacher P *et al*. (2008). Cannabinoids reduce markers of inflammation and fibrosis in pancreatic stellate cells. *PLoS One* **3**: e1701.

Michalski CW, Shi X, Reiser C, Fachinger P, Zimmermann A, Buchler MW *et al*. (2007b). Neurokinin-2 receptor levels correlate with intensity, frequency, and duration of pain in chronic pancreatitis. *Ann Surg* **246**: 786–793.

Michaud DS, Giovannucci E, Willett WC, Colditz GA, Stampfer MJ, Fuchs CS. (2001). Physical activity, obesity, height, and the risk of pancreatic cancer. *JAMA* **286**: 921–929.

Ohkubo I, Niwa M, Takashima A, Nishikimi N, Gasa S, Sasaki M. (1990). Human seminal plasma Zn-alpha 2-glycoprotein: its purification and properties as compared with human plasma Zn-alpha 2-glycoprotein. *Biochim Biophys Acta* **1034**: 152–156.

Roberts AB, Wakefield LM. (2003). The two faces of transforming growth factor beta in carcinogenesis. *Proc Natl Acad Sci USA* **100**: 8621–8623.

Robson EJ, Khaled WT, Abell K, Watson CJ. (2006). Epithelial-to-mesenchymal transition confers resistance to apoptosis in three murine mammary epithelial cell lines. *Differentiation* **74**: 254–264.

Rolli V, Radosavljevic M, Astier V, Macquin C, Castan-Laurell I, Visentin V *et al*. (2007). Lipolysis is altered in MHC class I zinc-alpha(2)-glycoprotein deficient mice. *FEBS Lett* **581**: 394–400.

Russell ST, Tisdale MJ. (2010). Antidiabetic properties of zinc-alpha2-glycoprotein in ob/ob mice. *Endocrinology* **151**: 948–957.

Russell ST, Zimmerman TP, Domin BA, Tisdale MJ. (2004). Induction of lipolysis *in vitro* and loss of body fat *in vivo* by zinc-alpha2-glycoprotein. *Biochim Biophys Acta* **1636**: 59–68.

Singh A, Greninger P, Rhodes D, Koopman L, Violette S, Bardeesy N *et al*. (2009). A gene expression signature associated with 'K-Ras addiction' reveals regulators of EMT and tumor cell survival. *Cancer Cell* **15**: 489–500.

Subramanian G, Schwarz RE, Higgins L, McEnroe G, Chakravarty S, Dugar S *et al*. (2004). Targeting endogenous transforming growth factor beta receptor signaling in SMAD4-deficient human pancreatic carcinoma cells inhibits their invasive phenotype1. *Cancer Res* **64**: 5200–5211.

Tada T, Ohkubo I, Niwa M, Sasaki M, Tateyama H, Eimoto T. (1991). Immunohistochemical localization of Zn-alpha 2-glycoprotein in normal human tissues. *J Histochem Cytochem* **39**: 1221–1226.

Von Burstin J, Eser S, Paul MC, Seidler B, Brandl M, Messer M *et al*. (2009). E-cadherin regulates metastasis of pancreatic cancer *in vivo* and is suppressed by a SNAIL/HDAC1/HDAC2 repressor complex. *Gastroenterology* **137**: 361–371.

Wan M, Huang J, Jhala NC, Tytler EM, Yang L, Vickers SM *et al*. (2005). SCF(beta-TrCP1) controls Smad4 protein stability in pancreatic cancer cells. *Am J Pathol* **166**: 1379–1392.

Wang Z, Li Y, Kong D, Banerjee S, Ahmad A, Azmi AS *et al*. (2009). Acquisition of epithelial-mesenchymal transition phenotype of gemcitabine-resistant pancreatic cancer cells is linked with activation of the notch signaling pathway. *Cancer Res* **69**: 2400–2407.

Zhang W, Erkan M, Abiatari I, Giese NA, Felix K, Kayed H *et al*. (2007). Expression of extracellular matrix metalloproteinase inducer (EMMPRIN/CD147) in pancreatic neoplasm and pancreatic stellate cells. *Cancer Biol Ther* **6**: 218–227.

Supplementary Information accompanies the paper on the Oncogene website (http://www.nature.com/onc)